2

Functional alkoxysilane mediated synthesis of Palladium nanoparticles and their role as Metal Enhanced Fluorescence or Fluorescent Resonance Energy Transfer platforms

---

2.1. INTRODUCTION

Nanoscaled Palladium is of specific significance as catalysts for various chemical reactions (Chung et al., 2002; Mubeen et al., 2007). Colloidal palladium has been widely investigated for its redox catalytic, photonic, optical and electrocatalytic properties in diverse practical applications (Jiang et al., 2009; Shen et al., 2013; Tang et al., 2016). The catalytic behavior of the metal is closely related to the structural properties like size, shape and composition. Hence, considerable efforts have been laid to tailor the morphological characteristics of the nanocrystals (Cheong et al., 2010; Tang and Cheng, 2015; Feng et al., 2018). Recent advancements in synthetic strategies have put forward a range of possibilities to precisely tune the nanostructures in order to obtain the material with desired functionality and structural orientations (Pei et al., 2018). In particular, a variety of palladium nanoparticles (PdNPs) of different shapes have been synthesized by a modified polyol reduction process (Xiong et al., 2005; Lee et al., 2010). Solution phase synthesis is suggested to be the most practical one among the different methods known for preparing the palladium nanocrystals (Shimizu et al., 2003, Quiros et al., 2002). Various conventional methods adopted for synthesizing the PdNPs, do not ensure the effective

stabilisation, monodispersibility and controlled morphological features. The present study deals with the wet chemical synthesis of PdNPs using organofunctionalised alkoxysilane 2-(3,4-epoxycyclohexyl) ethyltrimethoxysilane (EETMS).

2-(3,4-epoxycyclohexyl) ethyltrimethoxysilane (EETMS) has significant role in the construction of nanostructured matrix of organically modified silicates (ormosil) in combination with other alkoxysilanes like, 3-aminopropyltrimethoxysilane (APTMS), (Bartholome et al., 2005) 3-glycidoxypropyltrimethoxysilane (GPTMS) and trimethoxysilane (TMS). Ormosil provides the network for encapsulation of molecules like proteins (Avnir et al., 2006), redox coupling agents like ferrocene, potassium ferricyanide within nanostructured network, (Pandey et al., 2003) and also the electrocatalyst like palladium within the nanostructured mesh for electrochemical sensing applications (Pandey et al., 2001). APTMS has been arbitrarly used as stabilizing or capping agent in the presence of other reducing agents like GPTMS/cyclohexanone/THF-HPO/formaldehyde, for the controlled synthesis of functional noble metal nanoparticles like AuNPs, AgNPS and PdNPs in our previous reports (Pandey and Pandey, 2014). The micellar activity of APTMS and reducing nature facilitate in administering the dispersibility of as devised functional nanoparticles in diverse polar and non-polar solvents (Pandey et al., 2014). These findings unveiled the multiple applications of organically modified alkoxysilanes for yielding functional nanomaterials, either availing in homogeneous suspension or in heterogeneous nanostuctured matrix for focused applications. The organic functionalities linked to alkoxysilane not only add reactivity for above cited applications but also provide an excellent medium for the stabilization of *in situ* triggered metal nanoparticles. These findings directed us to investigate the

synthetic utility of EETMS (Jabbour et al., 2008; Briche et al., 2008) in order to fabricate the PdNPs with efficient morphological, compositional and catalytic properties.

The simple one step synthetic route to fabricate the monodisperse PdNPs, under the bifold action of alkoxysilanes (EETMS) and the polymeric stabilizer (PVP) has been demonstrated in the chapter. The role of epoxy moiety in reduction of palladium cations and stabilization of corresponding nanoscaled palladium atoms has been thoroughly investigated here. It has been anticipated that polymeric chain (PVP) acts as secondary stabilizer and together with EETMS supports the directional growth of particles (Cheong et al., 2010). Further, precise control over the concentration of precursors (EETMS and K_2PdCl_4), yielded the anisotropic palladium nanostructures, like nanocubes, nanoplates and other regular polyhedron nanocrystals (Lim et al., 2010; Berhault et al., 2007). The as-synthesised palladium nanocrystals are selected as substrates for metal-fluorophore interactions studies (Zhang et al., 2007; Zhuo et al., 2010).

The nanoscaled metal surfaces have been proved to influence the visual properties of the fluorophores (Zhang et al., 2010). The strength of Plasmon field of metal nanoparticles, experienced by the fluorophores, is responsible for the variations in fluorescence intensity (Vikovic et al., 2008). Variations (enhancement/quenching) in emission intensity are mainly driven by the effective distance at which flourophore is placed with respect to the metallic probe (Lakowicz, 2005; Lakowicz et al., 2008). The flouroscence enhancement (MEF) or quenching are known to occur as a result of converging factors like, increase in excitation rate of molecule due to the amplification in local electromagnetic field (Zhang et al., 2008), increase in decay rate due to coupling of plasmonic emission of metal nanoparticles with the fluorescence emission of the molecule, non radiative energy transfer from fluorophore to metal nanostructures, which is

also referred to as Fluorescence resonance energy transfer (FRET) (Cannone et al., 2006). Till now major findings on such investigation have been limited to metal nanoparticles with strong plasmonic activity (AuNPs, AgNPs), and for specific applications (Aslan et al., 2005; Skrabalak et al., 2007). The role of the functionalities in achieving the distance related effects between fluorophore and the nanocrystal surfaces has not been much pondered upon.

In this chapter, the EETMS functionalized anisotropic nanostructured palladium surfaces are used as effective substrates for analyzing the spectral fingerprints of different fluorophores (Rhodamine B, L-Tryptophan and Fluorescein) in liquid media based on the characteristic enhancement or quenching. The role of functional alkoxysilanes (EETMS, GPTMS and APTMS) as spacers between probe (Kedem et al., 2014) and the metal surfaces has been explored here, and are found to regulate this interspace phenomenon of fluorescence enhancement or quenching. Additionally, the results of the study are equated with other noble metal nanoparticles, AuNPs and AgNPs (Scheme 2.1) synthesized on the similar lines (Pandey et al., 2014; Pandey and Singh, 2015; Pandey and Pandey, 2016). The great enhancement is obtained for fluorescein in the presence of nanoparticles synthesized using APTMS.

2.2. EXPERIMENTAL

2.2.1. Materials

Potassium tetrachloropalladate (K_2PdCl_4), 2-(3,4-epoxycyclohexyl) ethyltrimethoxysilane (EETMS), 3-glycidoxypropyltriethoxysilane (GPTMS), 3-aminopropyltrimethoxysilane (APTMS) and polyvinylpyrrolidone (PVP), were purchased from Sigma–Aldrich. Tetrachloroauric acid and silver nitrate are obtained from HiMedia. Formaldehyde and methanol

were obtained from Merck, India. Millipore double distilled water was used for preparing all the aqueous solutions.

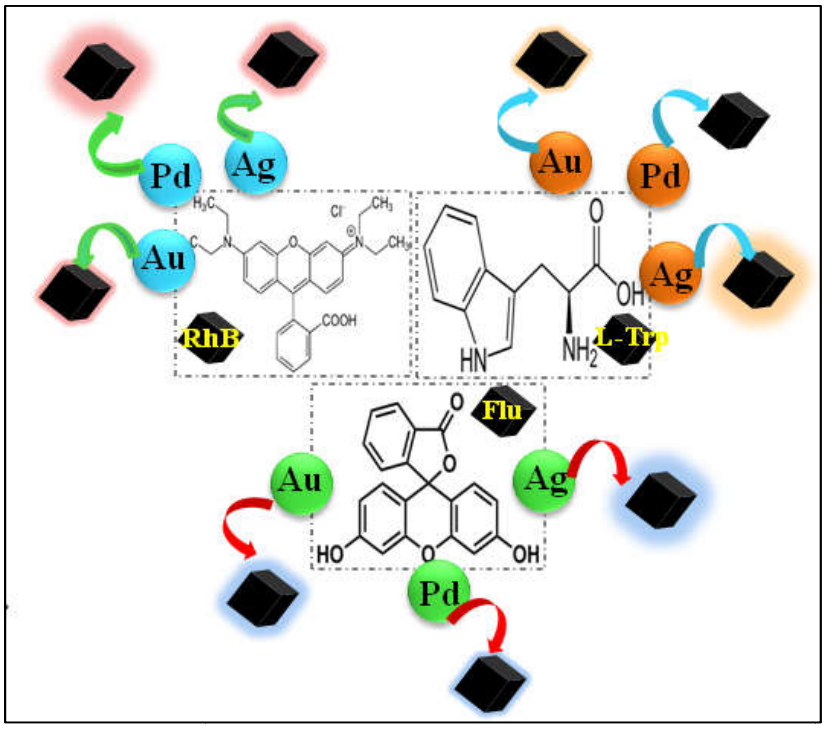

Scheme 2.1. Pictorial representation of the variation in fluorescence emission intensities with respect to the corresponding metal-fluorophore interactions.

2.2.2. EETMS/GPTMS mediated synthesis of palladium nanoparticles

Palladium nanoparticles with anisotropic structural properties were synthesized using wet chemical reduction pathway. First, the aqueous solutions of K_2PdCl_4 (2 – 10 mM, 1 mL) and PVP (1 %, 1 mL) were prepared. Secondly, the methanolic solutions of EETMS with concentration range (0.1 – 4.32 M) and GPTMS with concentrations 1 – 6 M were prepared. Next the solutions of K_2PdCl_4 (50 µL) and PVP (10 µL) were mixed, followed by the addition of EETMS (15 µL) of desired concentrations. Upon incubation for 10-15 minutes at 40-50 ºC, the

color of the mixture was changed to dark black, thus the EETMS based PdNPs were obtained. Further, the GPTMS based PdNPs were synthesized as follows: equal volume of the solutions of K_2PdCl_4 (50 μL) and GPTMS (50 μL) were mixed vigorously over the vertex cyclo mixer to yield brownish black colored palladium nanoparticles. Similarly, the APTMS/formaldehyde/GPTMS mediated gold and silver nanoparticles were synthesized using the protocols illustrated in our previous reports (Pandey and Singh, 2015; Pandey and Pandey, 2016).

2.2.3. Interaction of fluorophores with nanoarrays

Freshly prepared nanoparticles were utilized to formulate the samples for fluorescence survey. The samples were prepared by adding the solution of known concentrations of the fluorophores to the nanoparticle suspensions in a fixed ratio, and the resulting mixtures were diluted to 500 μL using methanol, followed by sonication for about 10 minutes. Further, the solutions were incubated for about 2-3 hours in dark under ambient conditions, followed by recording the fluorescence. The basic methanolic solutions of Fluorescein and L-Tryptophan, aqueous solution of Rhodamine B, of known concentration (10^{-7} M) were used for the study.

(a) With PdNPs

The three different types of mixtures of each type of fluorophore and PdNPs are prepared. (a) Fluorophore and Pd/EETMS, where the concentration of EETMS is kept constant (2.5 M) while the K_2PdCl_4 is varied over the range 2-20 mM, (b) Fluorophore and Pd/EETMS, where the concentration of EETMS is varied from 0.1 – 4.32 M, at constant K_2PdCl_4 (10 mM),

(c) Fluorophore and Pd/GPTMS, where the concentration of GPTMS is varied from 1 – 6 M, at constant K_2PdCl_4.

(b) With AgNPs

The four different types of mixtures of each Fluorophore and AgNPs are prepared. (a) Fluorophore and Ag/APTMS, where the concentration of APTMS is kept constant (1 M), while the $AgNO_3$ is varied over the range 5 – 20 mM, (b) Fluorophore and Ag/APTMS, where the concentration of APTMS is varied from 0.5 – 5.41 M, at constant $AgNO_3$ (5 mM), (c) Fluorophore and Ag/APTMS, where the concentration of APTMS is varied from 0.5 – 5.41 M, at constant $AgNO_3$ (10 mM), (d) Fluorophore and Ag/GPTMS, where the concentration of GPTMS is 4 M, at constant $AgNO_3$ (10 mM).

(c) With AuNPs

The four different types of mixtures of each Fluorophore and AuNPs are prepared. (a) Fluorophore and Au/APTMS, where the concentration of APTMS is kept constant (2 M), while the $HAuCl_4$ is varied over the range 2 – 25 mM, (b) Fluorophore and Au/APTMS, where the concentration of APTMS is varied from 0.5 – 5.41 M, at constant $HAuCl_4$ (5 mM), (c) Fluorophore and Au/APTMS, where the concentration of APTMS is varied from 0.5 – 5.41 M, at constant $HAuCl_4$ (10 mM), (d) Fluorophore and Au/GPTMS, where the concentration of GPTMS is 4 M, at constant $HAuCl_4$ (10 mM).

2.2.4. Material Characterisation

Transmission electron microscopy (TEM, Technai G^2 with accelerating voltage 200 kV) was employed to evaluate the morphological features of as synthesized nanoparticles. The

absorption spectra of nanoparticles and the emission spectra of flourophores were recorded using UV spectrophotometer (HITACHI U-2900, Hitachi Hi-Tech technologies, Tokyo, Japan) and Fluorescence spectrophotometer (HITACHI F-7000). The emission spectra of the interaction of fluorophores with the nanoparticles were analysed using fluorescent microscopy. Dynamic light scattering (DLS) measurements were carried out using Malvern instruments in order to investigate the relation of selective hydrodynamic radius (R_H) with the distance related effects on fluorescence intensity variations. XPS information was obtained from KRATOS, Amicus instrument using Al anodes producing Kα X-rays.

2.3. RESULTS

2.3.1. Synthesis and characterization of nanoparticles

Burkhart and coworkers (1994) have broadly investigated the role of glycidyl moiety (GPTMS) in the reduction of palladium. Also the reactivity of glycidyl group in framing the Pd-linked ormosil has been thoroughly reviewed by our group in recent years (Pandey et al., 2001). Since the epoxy moiety of the glycidyl group significantly resembles with that of epoxycyclohexyl group in EETMS, and also both the silanes are lipophilic in character, therefore it was intended to investigate the reducing and stabilizing properties of EETMS. It was observed that the EETMS being a silane derivative undergoes a slow reaction to form palladium particles. Although EETMS functionalized PdNPs are stable but in the presence of a secondary stabilizer like long chain polymer (PVP), the growth of particles is found to be uniform, so the bifold action of EETMS and PVP yielded homogenous dispersions of colloidal palladium as evident from the electron microscopic results (Figure 2.1). The physical features of the particles like size, shape were found to be the exact function of EETMS composition. At constant Pd^{2+} and PVP

with low molar ratio of EETMS (0.01 M), several triangular and hexagonal Pd nanoparticles were observed with mean particle size 30.6 ± 11 nm (Figure. 2.1a). While increasing the molar ratio of EETMS (from 0.01-0.5 M), heterogeneity of the system was increased with the appearance of various pyramidal, cuboidal, icosahedral, multiple twined structures (Xiong et al, 2016; Sun et al., 2018); the aspect ratio of nanoparticles decreased at the same time (21 ± 11.2 nm). The icosahedral, cuboidal nanostructures and triangular nanoplates are formed in abundance at this molar ratio of EETMS (0.5 M), which means the surface energies of the nanoparticles are precisely controlled. Further, at higher concentration of EETMS (1.5 M), the particles seemed to grow in an ordered and aligned pattern Figure 2.1p), also the average diameter is observed to reduce (17.7 ± 6.3 nm). At even higher concentrations (2.5 M) a dramatic change in particle size and complete transformation in morphology is observed. There is ten-fold decrease in average particle daimeter (3.47 ± 1.64 nm), also the polyhedral configuration of nanocrystals, entirely transfigured to spherical structures (Figure 2.1). The GPTMS based PdNPs are nearly spherical in shape with average diameter 3.5 ± 0.5 nm and narrow particle size distribution (Figure 2.2).

Gold nanoparticles are rapidly synthesized using alkoxysilanes and organic reducing agents. APTMS capped gold cations are transformed to colloidal form on reduction by formaldehyde or GPTMS, to yield APTMS-AuNPs and APTMS-GPTMS-AuNPs (Pandey and Pandey, 2014; Pandey and Pandey, 2016). TEM images of APTMS (1 M) based AuNPs reveal the uniform nucleation and narrow particle size distribution with average diameter 5.93 ± 1.17 nm (Figure 2.3),while the mean size of APTMS-GPTMS based AuNPs is around 15-30 nm. The size of the nanoparticles is the exact function of the concentrations of APTMS, which means with the

increasing molarity of APTMS the size of nanoparticles are found to increase. Additionally, the morphology of both the types of AuNPs is noticed to be nearly spherical and well dispersed.

Silver nanostructures (AgNPs) are also predicted to bring out variations in fluorescence intensity. Here, AgNPs are easily synthesized via chemical reduction pathway using alkoxysilanes (APTMS, GPTMS) and mild reducing agent like formaldehyde (Pandey and Singh, 2015). TEM images of APTMS (1 M) – AgNPs, illustrate the formation of approximately spherical AgNPs with average diameter 8.37 ± 2.06 nm [Figure 2.3(f-h)] while the SAED pattern confirms the polycrystalline behavior (Figure 2.3i). The size of the nanocrystals varies linearly with the concentrations of the APTMS. Similarly, the average size of APTMS – GPTMS based AgNPs vary with the molarity of APTMS, on increasing the concentrations of APTMS (0.005 – 3 M) the average particle size varies from 4.23 to 20 nm, at constant GPTMS (4 M). The combined action of the two alkoxysilanes induces homogeneous nucleation and effectively stabilizes the nanoparticles.

Figure 2.4 shows the XPS spectrum of PdNPs, AuNPs and AgNPs. The spectra of PdNPs exhibits the usual Pd 3d doublet with peaks $3d_{5/2}$ and $3d_{3/2}$ at 335 and 340 eV respectively, showing the PdNPs are existing in zero valent state. Similarly, the XPS profile of AuNPs shows a doublet with peaks $4f_{7/2}$ and $4f_{3/2}$ at 83.8 and 88.3 eV and that of AgNPs display a typical doublet with peaks $3d_{5/2}$ and $3d_{3/2}$ obtained at 368 and 374 eV. The results confirm that nanoarrays are favourably synthesized in Pd^0, Au^0 and Ag^0 forms.

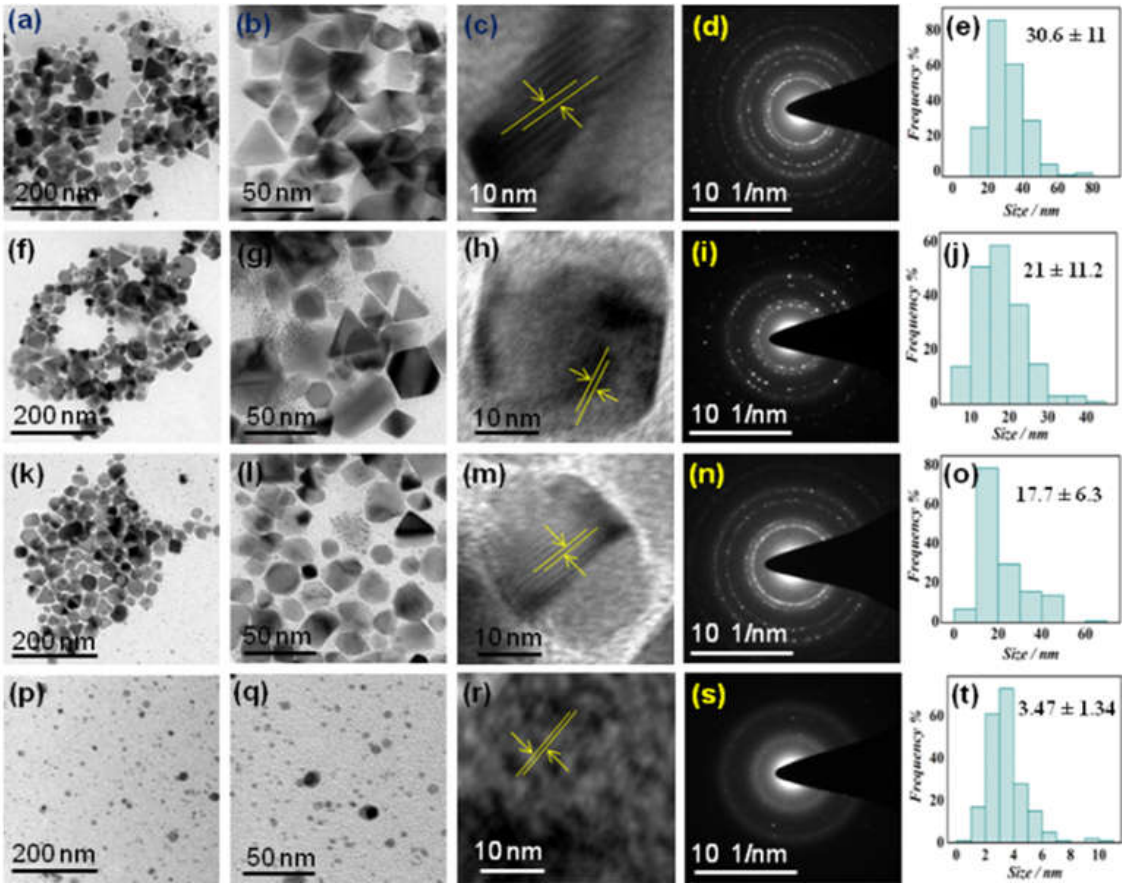

Figure 2.1. TEM images, SAED pattern and particle size distribution, of PdNPs arranged in increasing order of the concentration of EETMS, (a-e) 0.1 M, (f-j) 0.5 M, (k-o) 1.5 M, (p-t) 2.5 M.

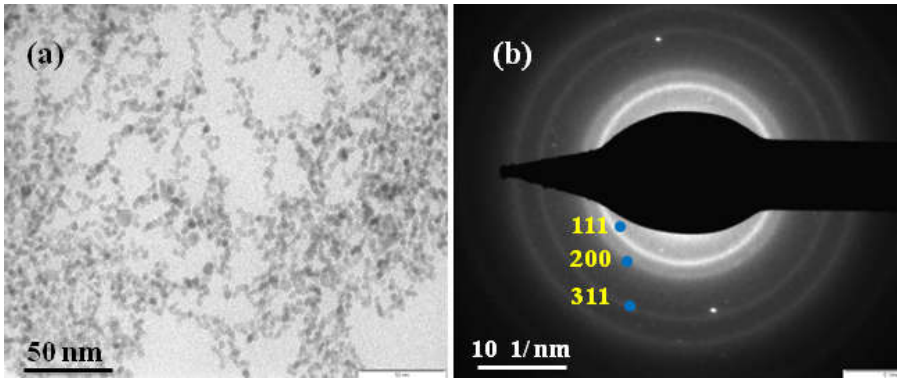

Figure 2.2. TEM image (a), SAED pattern (b) of PdNPs synthesized using GPTMS.

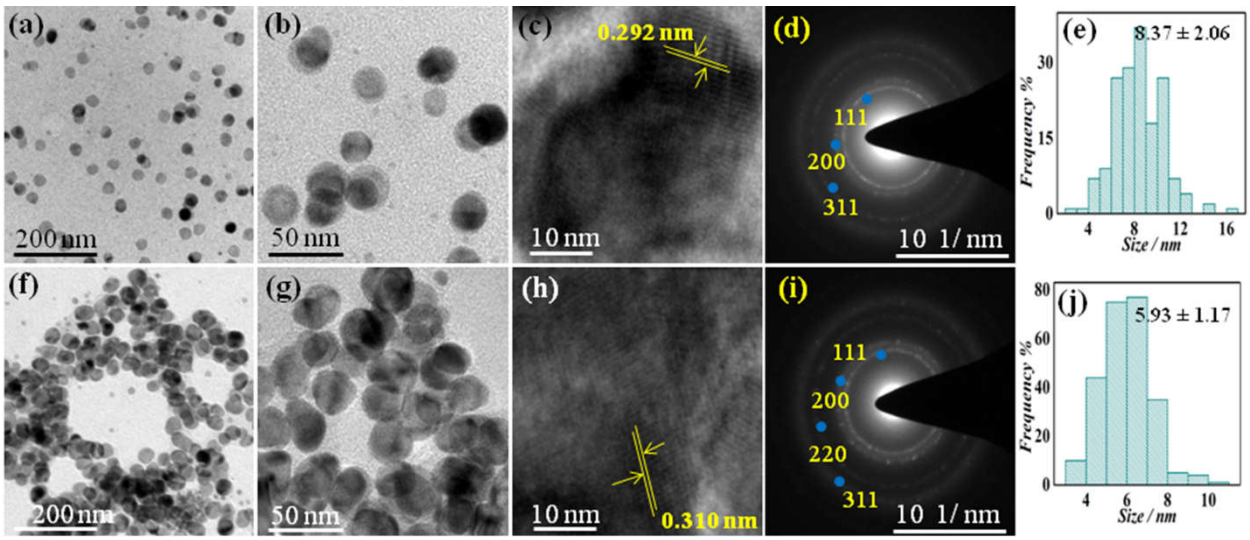

Figure 2.3. TEM images, SAED pattern and particle size distribution, of gold (a-e) and silver nanoparticles (f-j).

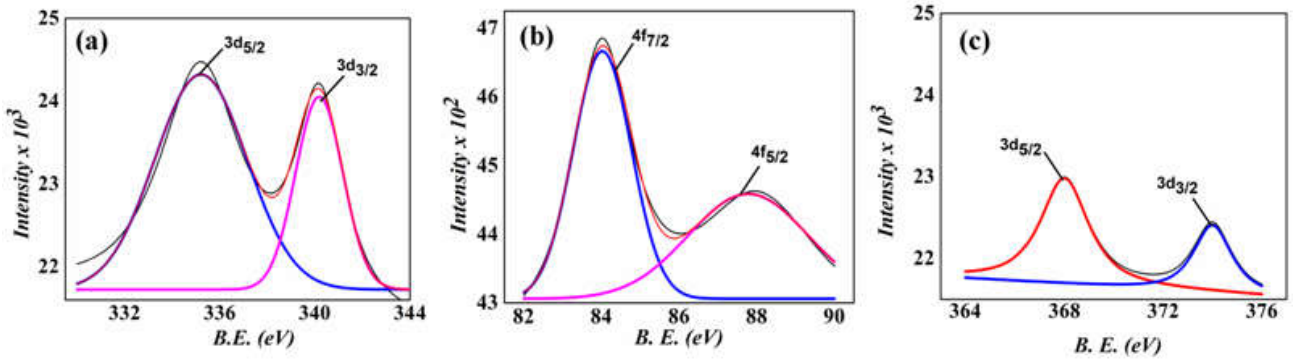

Figure 2.4. XPS profiles of monometallic (a) PdNPs, (b) AuNPs and (c) AgNPs.

2.3.2. Metal –Fluorophore Interactions

The interplay between the fluorophores (Fluorescein, Rhodamine B and L-Tryptophan) and the corresponding metal surfaces has been investigated comprehensively in this chapter. The variations in the emission intensity are observed to depend on the separation between the probe

molecules and the periphery of respective nanoparticles, which are synthesized using functionalized organosilane compounds. The layers of alkoxysilanes (EETMS, APTMS and GPTMS) act as spacers between fluorophores and the surface of nanocrystals (PdNPs, AuNPs and AgNPs), and control the thickness, which also prevent the superficial contact. These noble metal nanoarrays respond differently to different fluorophores (Figures 2.5-2.8).

2.3.2.1. Effect of Pd/EETMS and Pd/GPTMS systems on fluorescence intensity variations

The effect of palladium nanoparticle systems (Pd/EETMS and Pd/GPTMS) on the emission intensity of different fluorophores [Rhodamine B, Fluorescein and L-Tryptophan] has been recorded, as shown in Figures 2.5-2.8. Experimental results reveal that both the types of palladium nanocrystals show inconsistent response towards all the fluorophores.

(a) Influence of Pd/EETMS system on emission intensity of fluorophores

The extent of the interaction between probe molecules and EETMS based PdNPs vary according to the fluorophore. In case of the interplay between fluorescein (Flu) and PdNPs the emission intensity reached to a higher platform, when the concentration of EETMS was increased to 4.32 M (Figure 2.5). As shown in Figure 2.6, there was around 13.2 fold increase when molar concentration of EETMS was elevated to maximum (4.32 M) from 1 M. The significant enhancement in intensity was calculated using the relation I/I_0 (where, I and I_0 represent the fluorescence intensity of Flu in the presence and absence of Pd/EETMS). Further, remarkable 8.1 fold enhancement is observed at highest concentration of EETMS, which is clearly evident from the Figure 2.6. Rhodamine B (RhB) interacts differently with PdNPs (Figure 2.7), the emission intensity is enhanced over all the concentrations of EETMS (0.1-4.32 M).

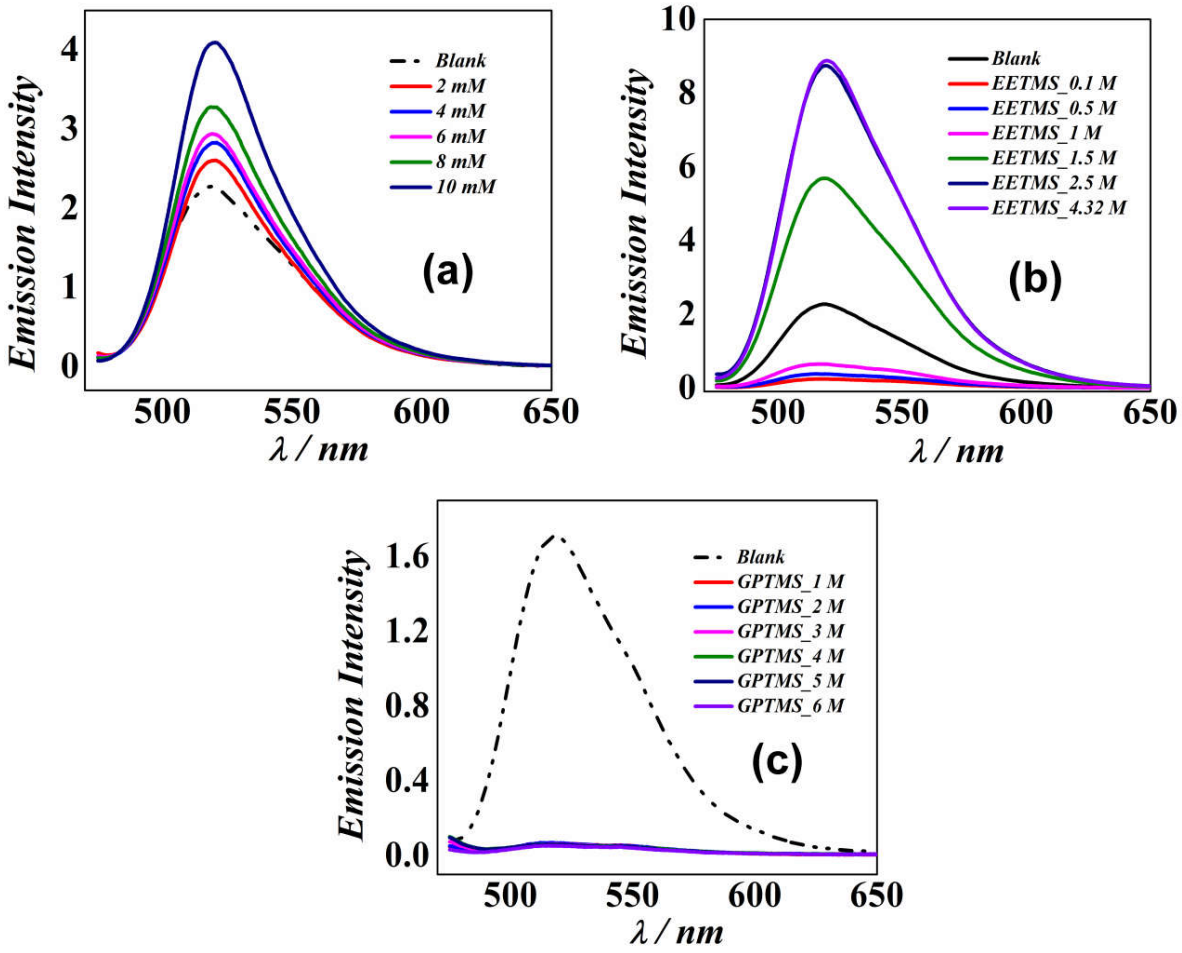

Figure 2.5. Fluorescence emission spectra of fluorescein in the presence of PdNPs. The variations in the emission intensity when (i) the concentration of K_2PdCl_4 is varied from 2 – 10 mM at constant EETMS, (ii) the EETMS is varied over the range 0.1 – 4.32 M and (iii) GPTMS is varied from 1 – 6 M, at constant K_2PdCl_4 (10 mM) for both (ii) and (iii).

Similarly, in case of L-tryptophan (L-Trp) and PdNPs interaction the fluorescence intensity was observed to be quenched (Figure 2.8). For the first few lower concentrations of EETMS, there was complete quenching, while on increasing the concentration to maximum (4.32 M), there was certain elevation that too was lower than the emission intensity I_0. Along with the variations in the intensity, shifts in emission maxima are also observed, also referred to as Stoke's and

Antistoke's shift. Additionally, the effect of variations in the concentration of palladium metal salt K_2PdCl_4 at constant EETMS (2.5 M) were also recorded in all the cases. A linear enhancement in emission intensity is observed with the increasing concentration of K_2PdCl_4 over the optimum range of 2-10 mM. Similar pattern is observed for Flu and RhB, while in case of L-Trp, quenching is recorded instead of enhancement.

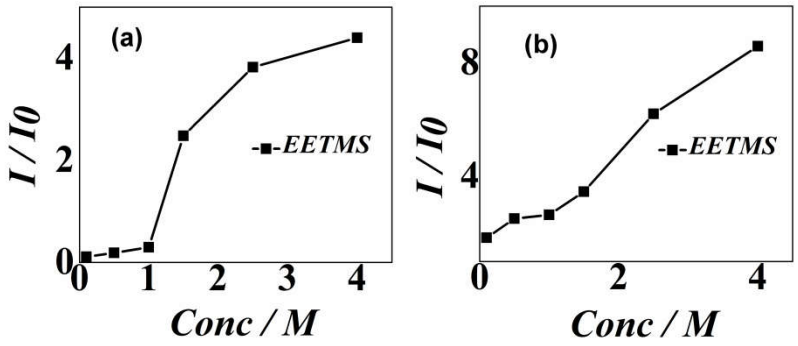

Figure 2.6. Plots of enhancement factor (EF) or fluorescence intensity change (I/I_0) with respect to the concentrations of EETMS, for the fluorophores (a) Rhodamine B and (b) Fluorescein.

(b) Influence of Pd/GPTMS system on emission intensity of fluorophores

The interaction of Flu with Pd/GPTMS results in complete quenching (Figure 2.5) at all the concentrations of GPTMS (1-6 M). Further, in case of L-Trp, the similar behavior was observed, there was complete quenching over the entire array of GPTMS concentrations. The interaction between RhB and Pd/GPTMS shows enhancement over the range of concentrations of GPTMS (1-6 M), but the emission intensity increases in the reverse order of the concentration of GPTMS, i.e., the maximum increase is noticed at the lowest amount of GPTMS and vice-versa.

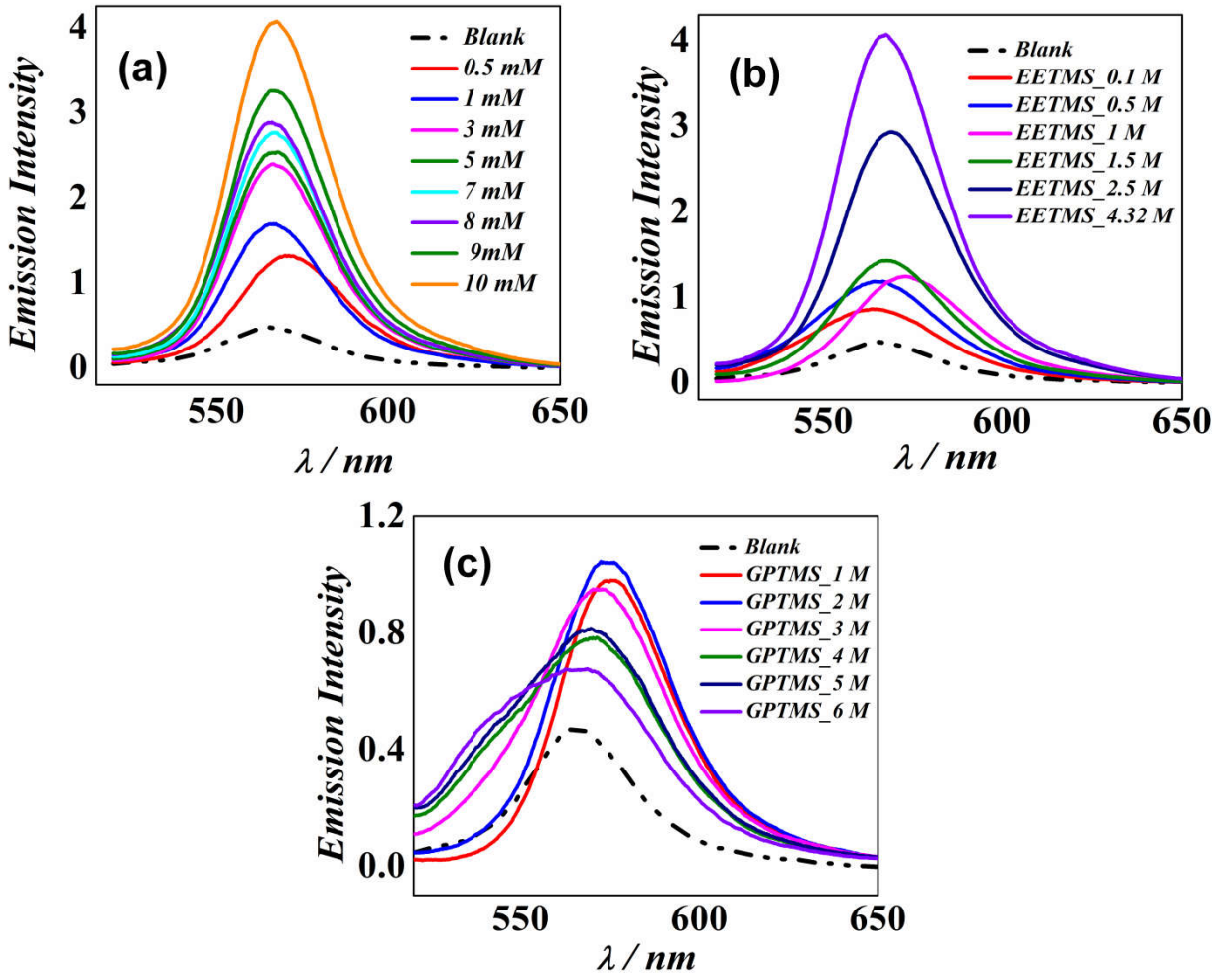

Figure 2.7. Fluorescence emission spectra of Rhodamine B in the presence of PdNPs. The variations in the emission intensity when (i) the concentration of K_2PdCl_4 is varied from 0.5 – 10 mM at constant EETMS, (ii) the EETMS is varied over the range 0.1 – 4.32 M and (iii) GPTMS is varied from 1 – 6 M, at constant K_2PdCl_4 (10 mM) for both (ii) and (iii).

2.3.2.2. Effect of APTMS and APTMS-GPTMS AuNPs on Fluorescence intensity variations

Gold nanoparticles are rapidly synthesized using alkoxysilanes and organic reducing agents. APTMS capped gold cations are transformed to colloidal form on reduction by formaldehyde or GPTMS, to yield APTMS-AuNPs and APTMS-GPTMS-AuNPs. The size of the nanoparticles is

the exact function of the concentrations of APTMS, which means with the increasing molarity of APTMS the size of nanoparticles are found to increase. Additionally, the morphology of both the types of AuNPs is noticed to be nearly spherical and well dispersed.

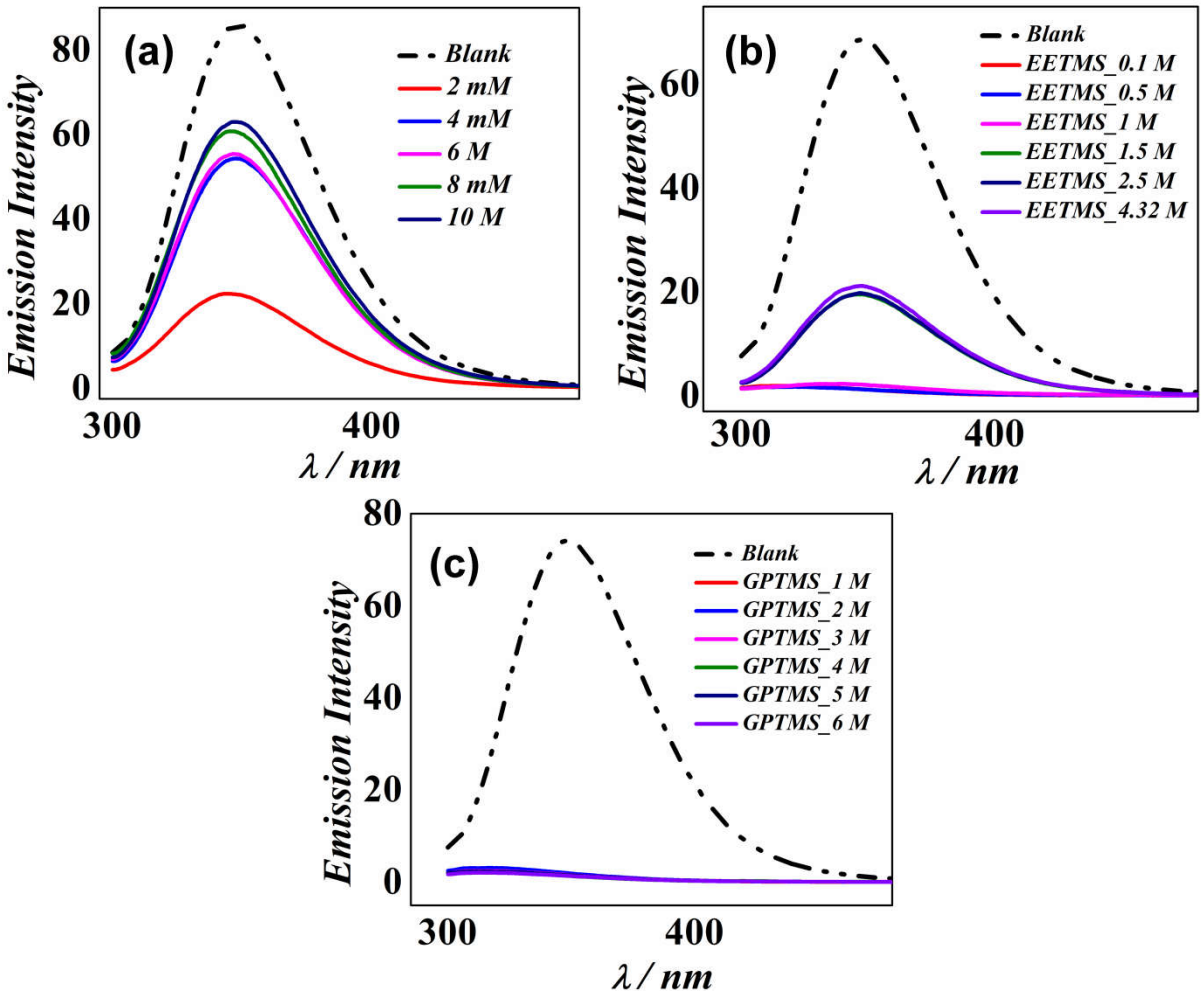

Figure 2.8. Fluorescence emission spectra of L-Tryptophan in the presence of PdNPs. The variations in the emission intensity when (i) the concentration of K_2PdCl_4 is varied from 0.5 – 10 mM at constant EETMS, (ii) the EETMS is varied over the range 0.1 – 4.32 M and (iii) GPTMS is varied from 1 – 6 M, at constant K_2PdCl_4 (10 mM) for both (ii) and (iii).

(a) Effect of APTMS-AuNPs system on emission intensity of fluorophores

Owing to the strong plasmonic activity of AuNPs, shows large spectral overlap with the fluorophores whose emission maxima lay close to the absorption band maxima of AuNPs (Bardhan et al, 2008). Thus the interaction of AuNPs with Fluorescein (λ_{em} = 518 nm) and Rhodamine B (λ_{em} = 525 nm) leads to significant enhancement in the emission intensity. The AuNPs and Fluorescein interact in a highly concentration depends on the concentrations of APTMS which is further regulated by the molar ratio of gold cation. Figure 2.9 shows, at the highest concentration of APTMS (5.41 M) and 10 mM $HAuCl_4$, the intensity was raised to 7.5 times to that in absence of AuNPs. Over the lower concentrations from 0.5-1.5 M APTMS, the intensity is greatly quenched, while on further increase (2-5.41 M), wide linear enhancement is observed. Similarly, at 20 mM of $HAuCl_4$, considerably different pattern of enhancement is observed. The intensity is appreciably quenched from 0.5 – 2.5 M APTMS, meanwhile, a dramatic 7 fold enhancement occurs at 3 M and 5.41 M APTMS. According to the previous reports on distance dependent variations in emission intensity, the enhancement decreases with the increasing concentrations of metal salt, the inferences from the present study are in agreement.

Further, the fluorescence intensity expectedly increases on interaction of AuNPs and Rhodamine B. A linear enhancement is observed over the range of concentration of APTMS (0.5 – 5.41 M), with around 7.4 fold increase at the highest concentration (5.41 M). As discussed in Fluorescein – AuNPs case, the enhancement follows the identical order, i.e., there was only 4 fold increase in intensity at 20 mM $HAuCl_4$ as compared to 10 mM with 7.4 fold growth.

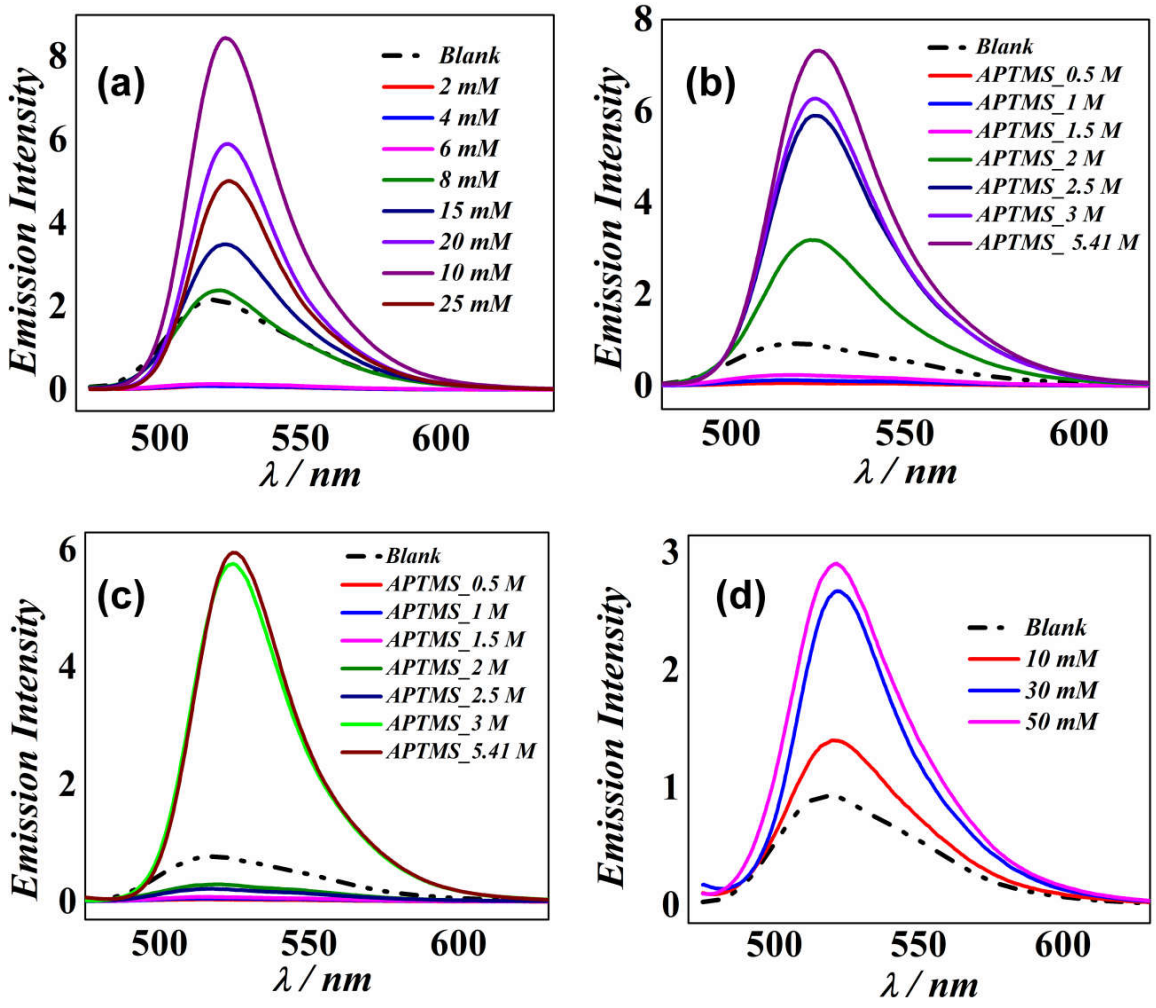

Figure 2.9. Fluorescence emission spectra of Fluorescein in the presence of AuNPs. The variations in the emission intensity when (i) the concentration of $HAuCl_4$ is varied from 2 – 25 mM at constant APTMS, (ii) the APTMS is varied over the range 0.5 – 5.41 M at constant $HAuCl_4$ (10 mM) (iii) the APTMS is varied over the range 0.5 – 5.41 M at constant $HAuCl_4$ (10 mM) (iv) the concentration of $HAuCl_4$ is varied from 10 – 50 mM at constant GPTMS.

Moreover, AuNPs quench the fluorescence of L-Tryptophan, over all the concentrations of APTMS (0.5 – 5.41 M) as shown in Figure 2.11. Here plasmonic modes of AuNPs do not effectively overlap with the emission maxima (λ_{em} = 350 nm) of L-Tryptophan. Furthermore, the effect of the variation of the concentration of $HAuCl_4$ (2 – 25 mM) at constant APTMS (2 M) is

also explored, in order to understand the behavior of the fluorophores with respect to the number of nanoparticles present in the mixture. Acute enhancement in intensity is observed in case of fluorescein – AuNPs, over the broad concentration range. Similarly, the intensity grew linearly for RhB-AuNPs system with proportional increase in concentrations (Figure 2.12). However, the prominent quenching has been detected for the L-Trp – AuNPs system over the range of variable concentrations of $HAuCl_4$ (2 – 25 mM).

(b) Influence of APTMS-GPTMS-AuNPs system on emission intensity of fluorophores

In the present alkoxysilane dependent investigation, yet another type of AuNPs prepared using the twin properties of two alkoxysilanes namely APTMS and GPTMS. The dynamics of reciprocity between these AuNPs and the respective fluorophores, follows different line of interaction in contrast to the above category (APTMS-AuNPs). The emission intensity is observed to increase with increasing concentrations of $HAuCl_4$ (10 – 50 mM) at constant GPTMS (4 M) and APTMS (2 M), about 3 fold amplification is recorded.

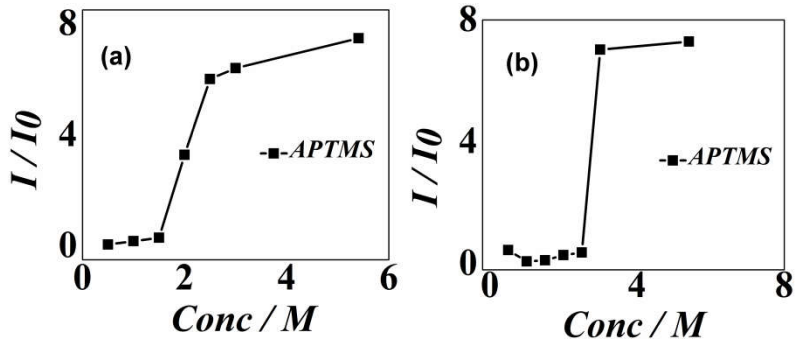

Figure 2.10. Plots of enhancement factor (EF) or fluorescence intensity change (I/I_0) with respect to the concentrations of EETMS, for the Fluorescein at (a) 10 mM and (b) 20 mM $HAuCl_4$.

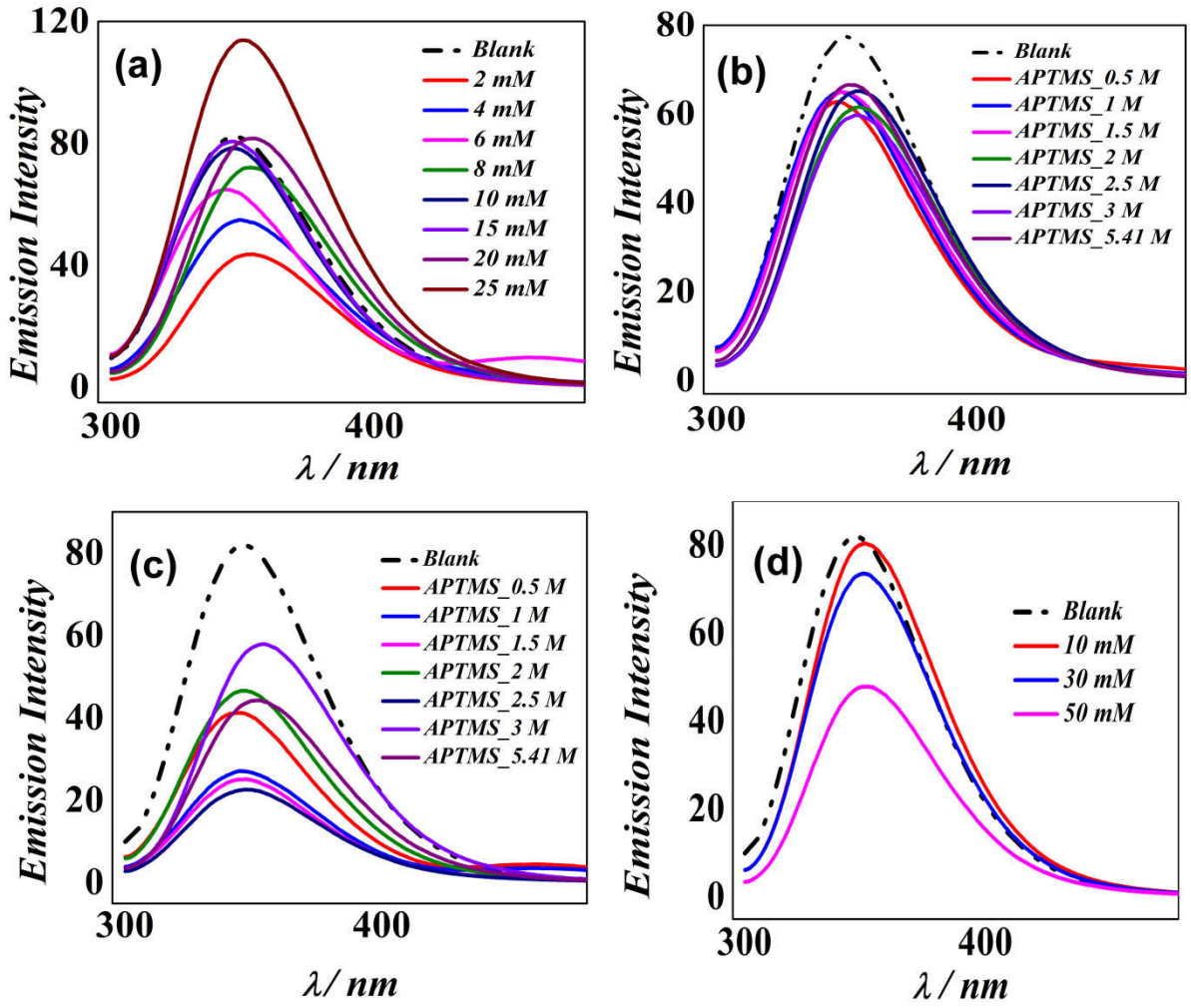

Figure 2.11. Fluorescence emission spectra of L-Tryptophan in the presence of AuNPs. The variations in the emission intensity when (i) the concentration of $HAuCl_4$ is varied from 2 – 25 mM at constant APTMS, (ii) the APTMS is varied over the range 0.5 – 5.41 M at constant $HAuCl_4$ (10 mM) (iii) the APTMS is varied over the range 0.5 – 5.41 M at constant $HAuCl_4$ (10 mM) (iv) the concentration of $HAuCl_4$ is varied from 10 – 50 mM at constant GPTMS.

3Similar sequence is followed for the RhB – AuNPs system and around 6.2 fold magnification is achieved (Figure 2.13). However, in case of L-Trp – AuNPs the intensity is considerably quenched over all the concentrations.

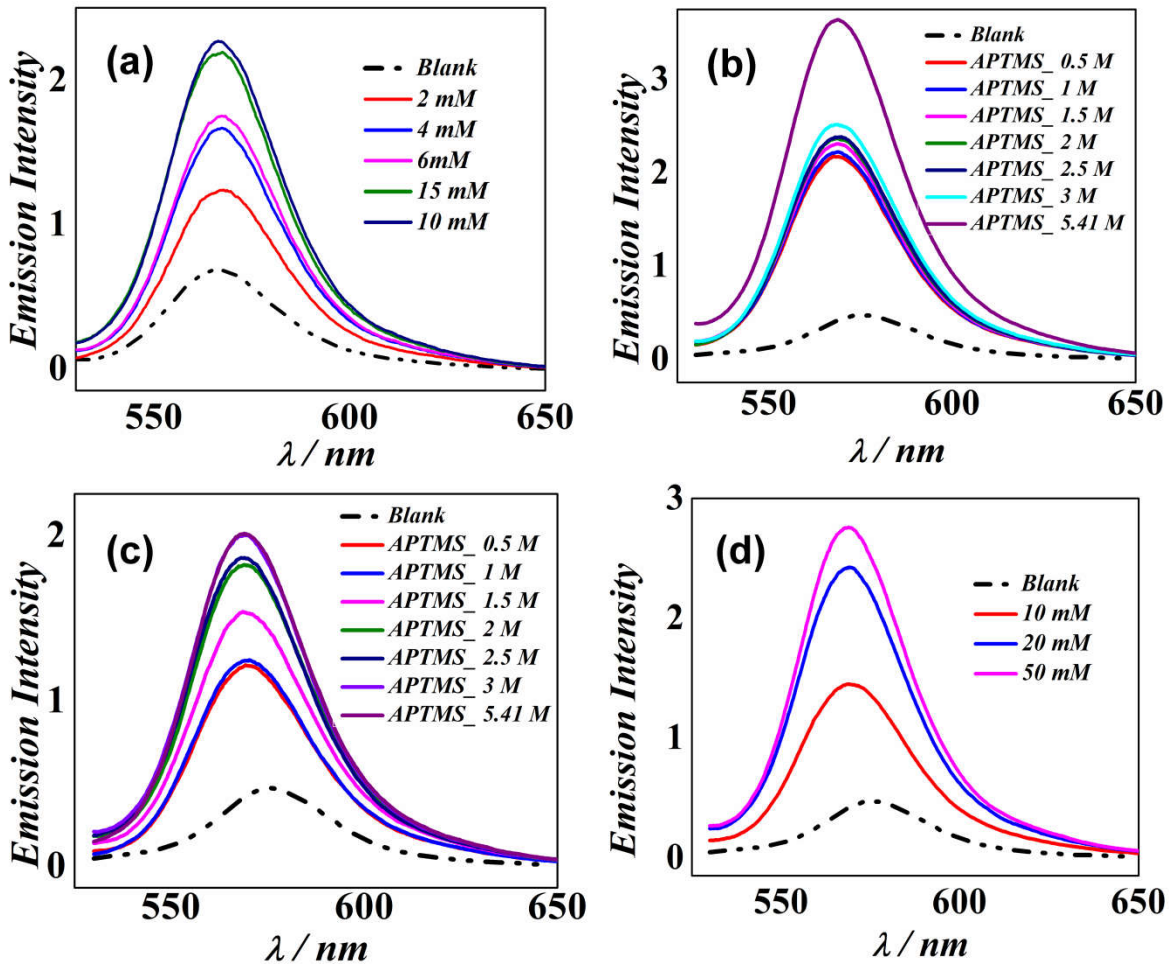

Figure 2.12. Fluorescence emission spectra of Rhodamine B in the presence of AuNPs. The variations in the emission intensity when (i) the concentration of $HAuCl_4$ is varied from 2 – 25 mM at constant APTMS, (ii) the APTMS is varied over the range 0.5 – 5.41 M at constant $HAuCl_4$ (10 mM) (iii) the APTMS is varied over the range 0.5 – 5.41 M at constant $HAuCl_4$ (10 mM) (iv) the concentration of $HAuCl_4$ is varied from 10 – 50 mM at constant GPTMS.

2.3.2.3. Effect of APTMS and APTMS-GPTMS AgNPs on Fluorescence intensity variations

Silver nanostructures (AgNPs) are also predicted to bring out variations in fluorescence intensity. In the context of metal enhanced fluorescence, earlier reports suggest that silver island films deposited on glass slides work as efficient substrates. Indeed, analyses of targeted fluorophores in homogenous liquid media give additionally significant results as discussed here.

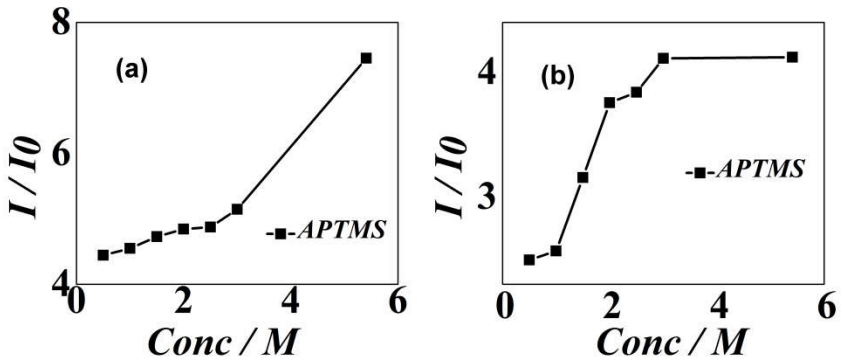

Figure 2.13. Plots of enhancement factor (EF) or fluorescence intensity change (I/I_0) with respect to the concentrations of APTMS, for the Rhodamine B at (a) 10 mM and (b) 20 mM $HAuCl_4$.

(a) Influence of APTMS-AgNPs system on emission intensity of fluorophores

Unusual effects on the emission intensities are demonstrated upon loading the fluorophores (Fluorescein, RhB and L-Trp) in proximity with AgNPs in solution phase (Figures 2.14-2.19). The fluorescence intensity is raised to 13.5 times when AgNPs interact with fluorescein. For the first few lower concentrations of APTMS (0.5 – 1 M), the intensity is greatly quenched, but at higher ones (1.5 – 5.41 M), it steadily progresses to enhancement (Figure 2.14-2.15). Similar variations in intensity are recorded over the range of concentrations of APTMS (0.5 – 5.41 M), when 10 mM $AgNO_3$ is administered for the AgNPs synthesis, except no further enhancement was recorded above 3 M APTMS. Further, AgNPs are observed to interact exceptionally well with L-Tryptophan, probably due to the effective overlap of the absorption (λ_{max} = 378 - 400 nm) and emission maxima (λ_{em} = 350 nm) of AgNPs and L-Tryptophan (Figure 2.16). The emission intensity reached the higher platform with subsequent increase in the APTMS content and almost no quenching has been spotted when 5 mM $AgNO_3$ has been used. A regular enhancement is observed (Figure 2.18) with proportional increase in APTMS (0.5 – 5.41 M). While quenching is

recorded when the analysis is done using the 10 mM $AgNO_3$ based AgNPs, where intensity is enhanced only at two higher concentrations of APTMS (3 and 5.41 M).

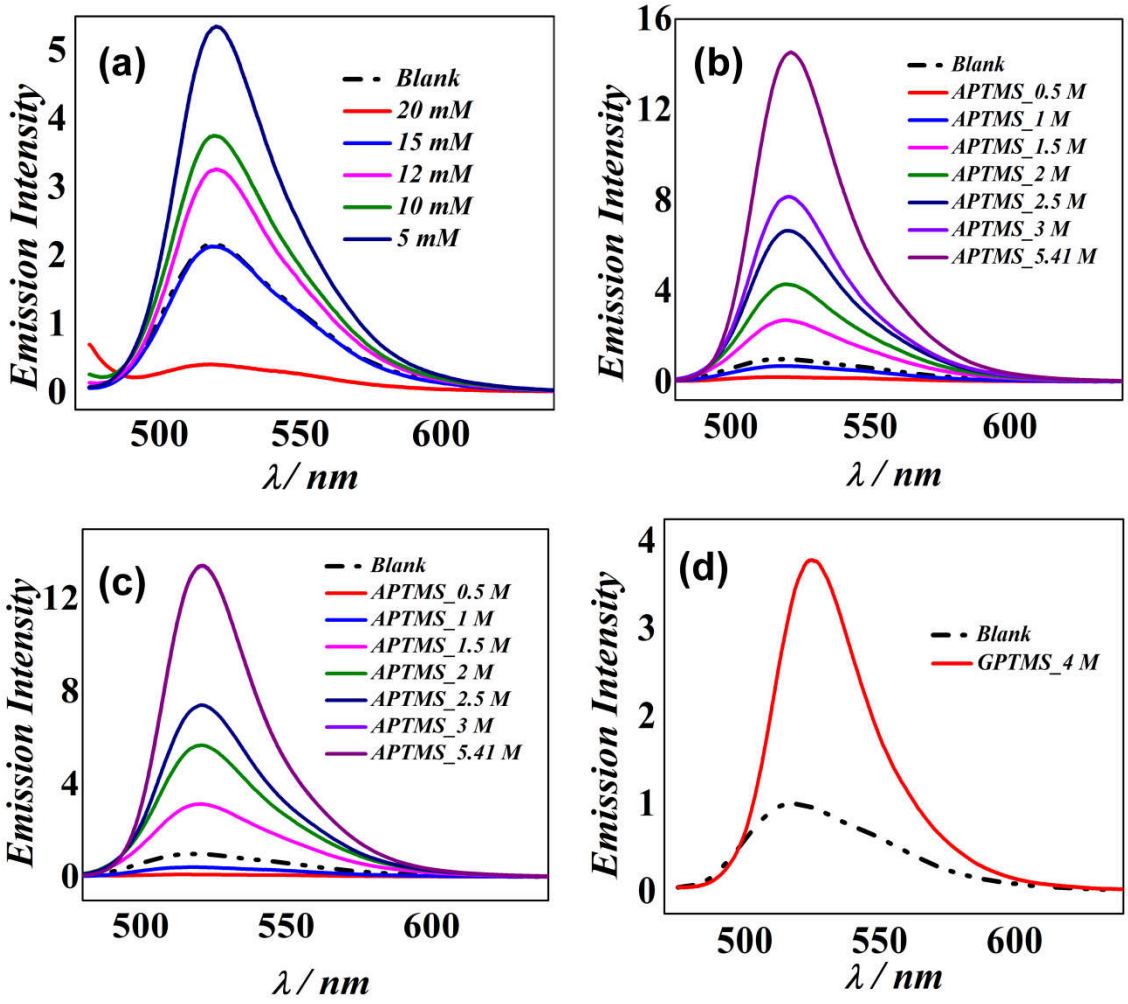

Figure 2.14. Fluorescence emission spectra of Fluorescein in the presence of AgNPs. The variations in the emission intensity when (i) the concentration of $AgNO_3$ is varied from 5 – 20 mM at constant APTMS, (ii) the APTMS is varied over the range 0.5 – 5.41 M at constant $AgNO_3$ (5 mM) (iii) the APTMS is varied over the range 0.5 – 5.41 M at constant $AgNO_3$ (10 mM) (iv) at constant 4 M GPTMS.

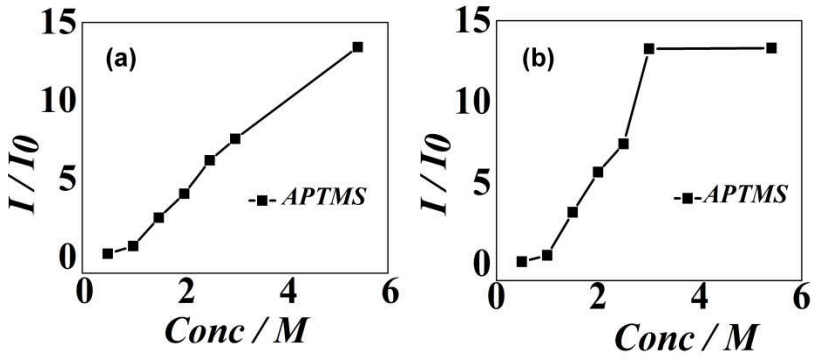

Figure 2.15. Plots of enhancement factor (EF) or fluorescence intensity change (I/I_0) with respect to the concentrations of APTMS, for the Fluorescein at (a) 5 mM and (b) 10 mM $AgNO_3$.

Furthermore, the interaction between AgNPs and RhB (Figure 2.17) result in around 6 fold enhancement (Figure 2.19) in emission intensity at all the concentrations of APTMS (0.5 – 5.41 M). Additionally, an attempt has also been made to investigate the effect of change in the concentrations of precursor metal salt ($AgNO_3$, 5 – 20 mM).

(b) Influence of APTMS-GPTMS-AgNPs system on emission intensity of fluorophores

The interaction of another type of AgNPs, prepared using consolidated action of two alkoxysilanes (APTMS and GPTMS) with different properties. This type of AgNPs interacts differently with the Fluorophores. With Fluorescein around 3 fold enhancement is recorded, which is quite low as compared to the above type. Further, in case of L-Tryptophan-AgNPs, quenching is observed. The trend with RhB is quite similar to that obtained for above system (APTMS-AgNPs), but only 2.8 fold enhancement is recorded.

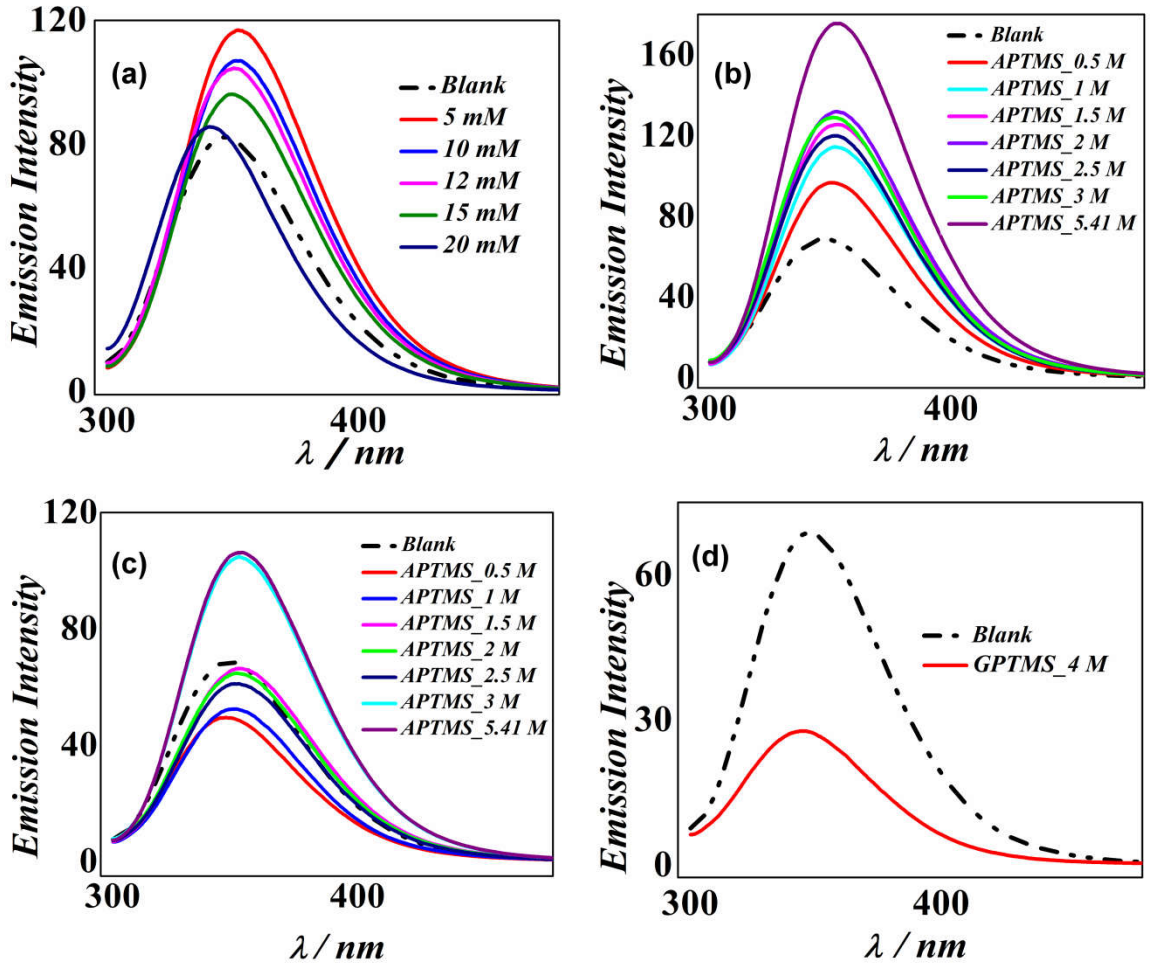

Figure 2.16. Fluorescence emission spectra of L-Tryptophan in the presence of AgNPs. The variations in the emission intensity when (i) the concentration of $AgNO_3$ is varied from 5 – 20 mM at constant APTMS, (ii) the APTMS is varied over the range 0.5 – 5.41 M at constant $AgNO_3$ (5 mM) (iii) the APTMS is varied over the range 0.5 – 5.41 M at constant $AgNO_3$ (10 mM) (iv) at constant 4 M GPTMS.

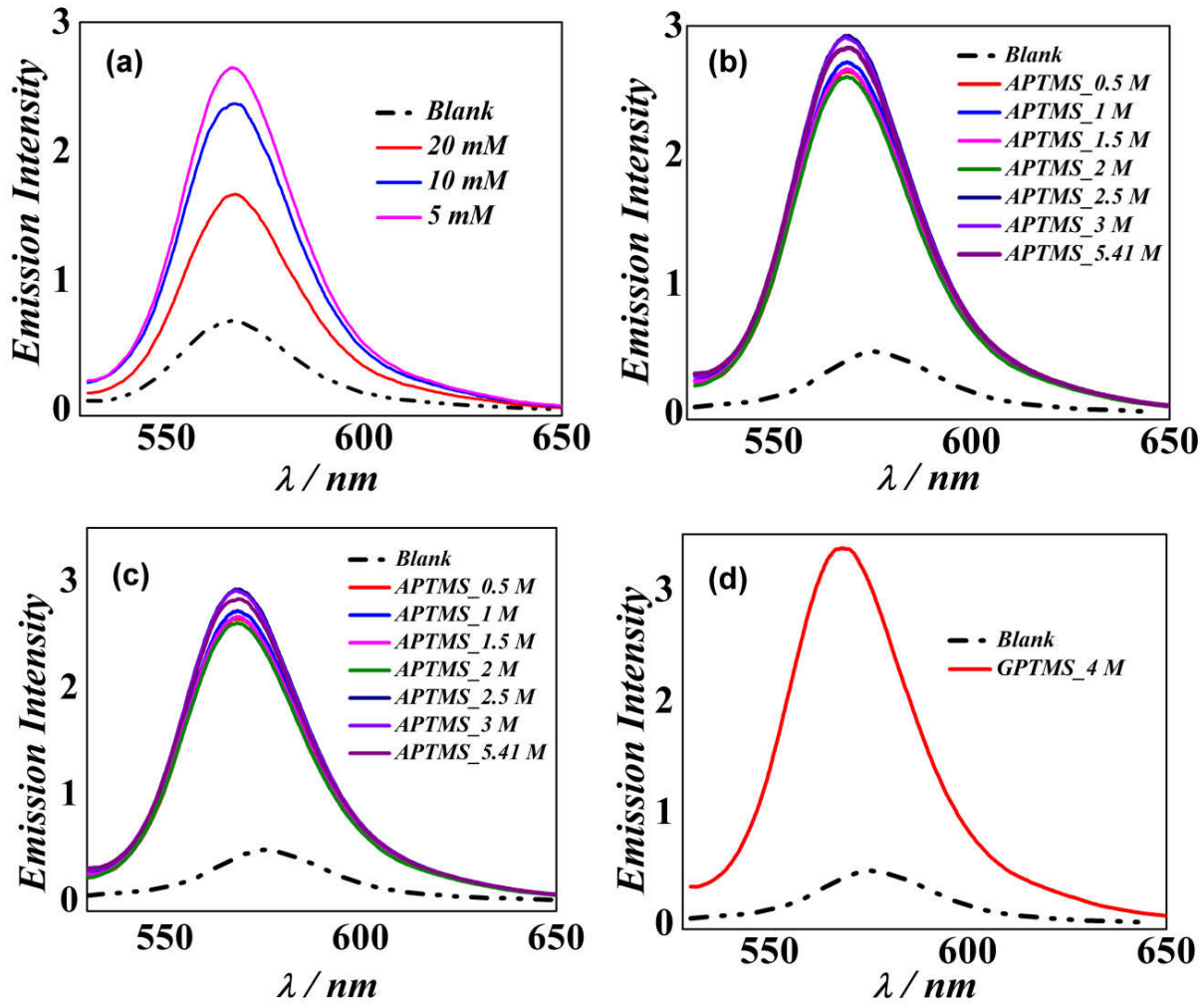

Figure 2.17. Fluorescence emission spectra of Rhodamine B in the presence of AgNPs. The variations in the emission intensity when (i) the concentration of $AgNO_3$ is varied from 5 – 20 mM at constant APTMS, (ii) the APTMS is varied over the range 0.5 – 5.41 M at constant $AgNO_3$ (5 mM) (iii) the APTMS is varied over the range 0.5 – 5.41 M at constant $AgNO_3$ (10 mM) (iv) at constant 4 M GPTMS.

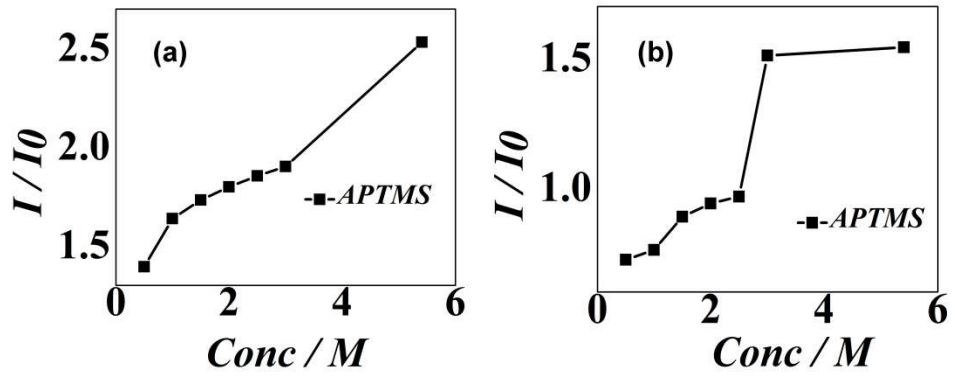

Figure 2.18. Plots of enhancement factor (EF) or fluorescence intensity change (I/I_0) with respect to the concentrations of APTMS, for the L-Tryptophan at (a) 5 mM and (b) 10 mM $AgNO_3$.

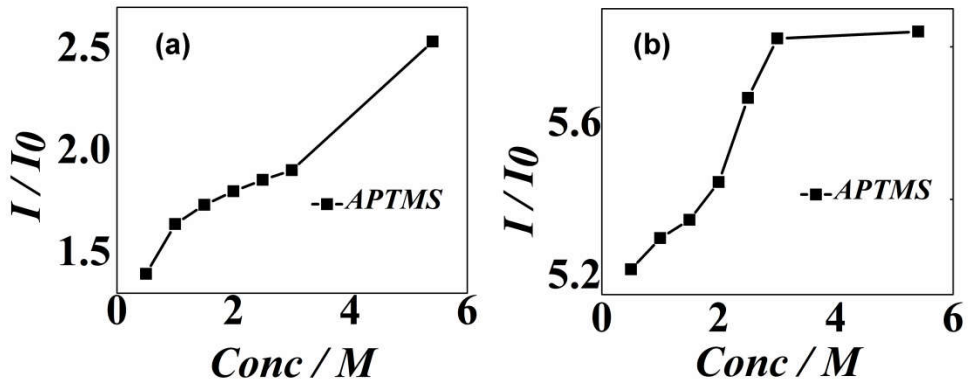

Figure 2.19. Plots of enhancement factor (EF) or fluorescence intensity change (I/I_0) with respect to the concentrations of APTMS, for the Rhodamine B at (a) 5 mM and (b) 10 mM $HAuCl_4$.

2.4. DISCUSSION

2.4.1. Role of EETMS in fabrication of palladium nanoparticles

The synergistic behavior of PVP and the controlled concentrations of EETMS yielded uniformly distributed anisotropic palladium nanoparticles. The liphophilic nature of EETMS stimulated the slower reduction rate for promoting the directional growth of the nanoparticles where aspect

ratio of corresponding particles depend on the concentration of precursors. It is known that under weak reducing conditions, higher concentration of monomers is formed and the reaction is kinetically controlled (Cheong et al., 2010). Therefore, on reduction using EETMS, the nucleation is slow in early stages, due to which the growth of nanoparticle is precisely controlled in later stages (Lee et al., 2010). The fate of reaction between reductant (EETMS) and metal precursor has been possibly understood by the mechanism proposed in Scheme 2.2.

The reaction is based on typical lewis-acid base interaction between Pd^{2+} (lewis acid) and epoxy moiety of the functionalized alkoxysilane (EETMS), to yield black colored colloidal solution of palladium nanoparticles. Mechanism of the reaction was validated using the FTIR measurements. The formation of olefin derivative and absence of the epoxide linkage in the product is reasonably justified from the IR spectra (Figure 2.20), appearance of a strong peak at 1642–1646 cm^{-1} in (2) indicated the presence of C-C while rest of the peaks determine the presence and absence of epoxy linkage in reductant and final byproduct.

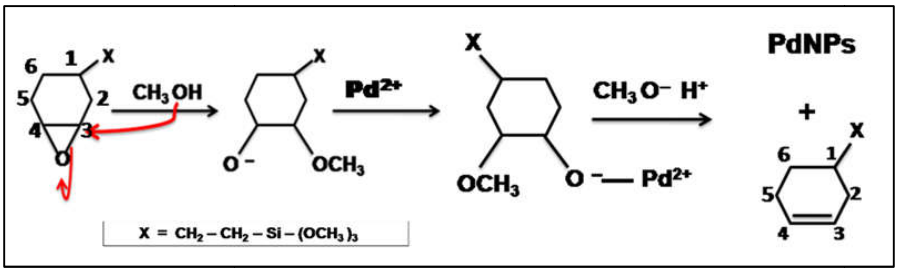

Scheme 3.2. Proposed mechanism for 2-(3, 4-epoxycyclohexyl)ethyltrimethoxysilane mediated synthesis of palladium nanoparticles.

The TEM images of PdNPs (Figure 2.1) show a complete transformation from regular polyhedral structures to approximately spherical. The molar ratios of EETMS play a crucial role in

controlling the morphologies. SAED patterns acknowledge the decrease in crystallinity of the nanoparticles as a function of EETMS concentration.

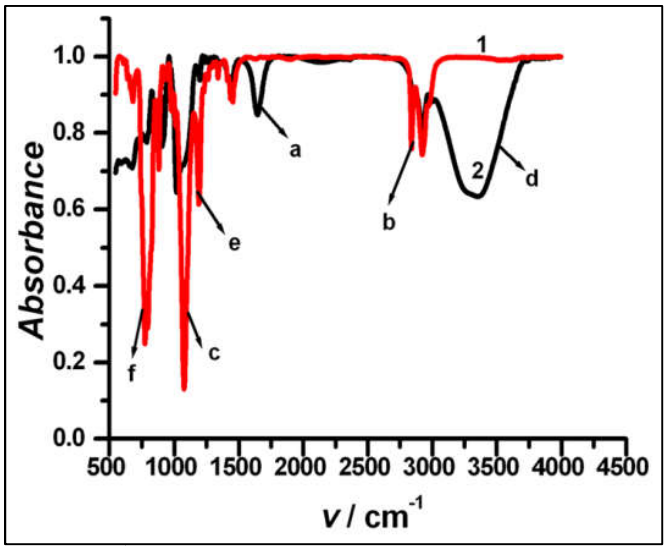

Figure 2.20. Infrared spectra of 2-(3-4,Epoxycyclohexyl)ethyltrimethoxysilane (1) and Palladium nanoparticle dispersion (2) with major peaks at (a) 1642 cm^{-1} (s; C – C), (b) 2920 cm^{-1} (C–H), (c) 1087 cm^{-1} (s; Si–O), (d) 3400 cm^{-1} (O – H) (e) 1190 cm^{-1} (epoxy ring), (f) 891 cm^{-1} (s (epoxy ring)), respectively.

2.4.2. Effect of alkoxysilanes on metal nanoparticle and fluorophore interactions

Organofunctionalised alkoxysilanes, EETMS, APTMS and GPTMS form the shell around individual particles and support the physisorption of probe molecules, which also prevents the aggregation by increased interparticle repulsions. Together with PVP, silane derivatives work as fluorescence tag for the adsorption of fluorophores and also the further desorption of probe molecules is restricted. The variations in the fluorescence emission intensity are found to be closely related to the concentration of alkoxysilanes (Figures 2.5-2.19). Here the alkoxysilanes are responsible for regulating the distance related effects on fluorescence. As evident from the

dynamic light scattering (DLS) results (Figure 2.21), the enhancement in emission is associated with the larger separations (around 350 nm) between the fluorophore and the metal surfaces.

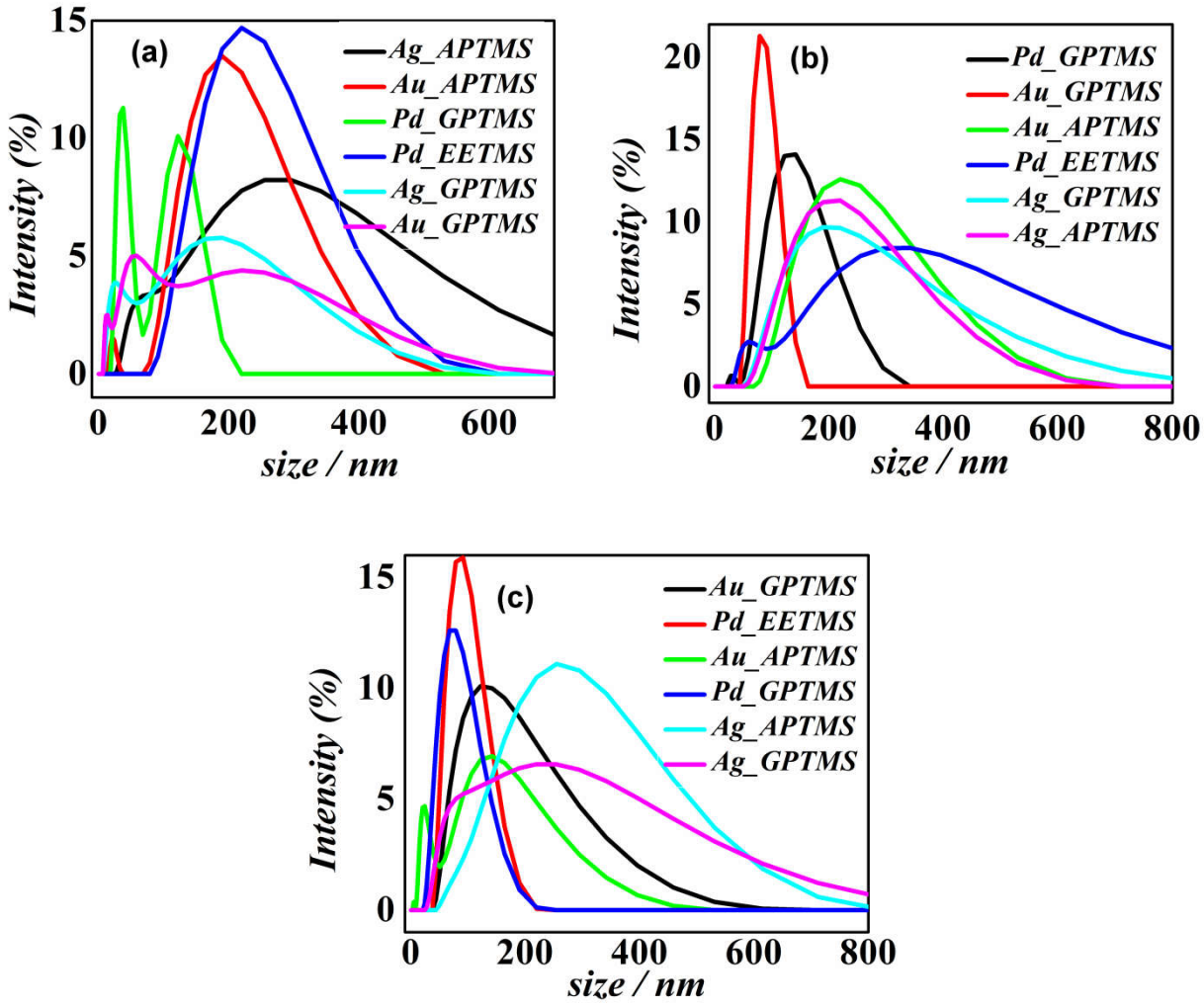

Figure 2.21. DLS profiles of the variations in hydrodynamic radii (R_H) on the interaction between the alkoxysilane functionalized nanoparticles and the corresponding flourophores (a) Fluorescein, (b) Rhodamine and (c) L-Tryptophan.

There is a competition between the enhancement and quenching processes, which are sharply linked to the spacer thickness. The non radiative energy transfer is mainly observed for the systems with low hydrodynamic radii (R_H), while those with higher R_H value promote the

enhancement in intensity. The interactions of different probe molecules with Pd/GPTMS system reportedly shows suppression or quenching of emission intensity, due to the close separation, which is below 150 nm. For the APTMS based systems the enhancement is found to depend on the metal and the type of fluorophore (molecular size, emission maxima). Owing to the smaller size of L-Tryptophan molecule the hydrodynamic radii appears to decrease for most of the systems, therefore quenching is observed for all the types of metal spacer combinations, except that of silver based system (Ag/APTMS).

According to the DLS results, variations in intensities of emission signals totally depend on the photophysical and chemical properties of alkoxysilanes, which are acting as spacers in the present investigations. The amphiphilic nature of APTMS led to the formation of micellized phase on large silver nanostructures which further facilitated the self assembly of particles, when localized with oscillating dipolar species, particularly fluorescein where stoke's shift is larger corresponding to the AgNPs. Moreover, the degree of adsorption of different flourophores on silver substrates is higher in case of Ag/APTMS, which supported the higher excitation efficiency and signal amplification. Other alkoxysilanes being hydrophobic do not support the creation of micellar phase and thus the separation between probe molecule and particle surface is not ordered, resulting in non radiative energy transfer.

In general, the enhancement is particularly recorded in case of fluorescein and Rhodamine B with different metal-alkoxysilane fusions. Due to the large molecular sizes of these fluorophores, separations with the metal surfaces remain favourably controlled, which often resulted in enhancement. Therefore, in this chapter, we have demonstrated the alkoxysilane (APTMS, EETMS and GPTMS) dependent changes in fluorescence intensity apart from the nature of metal

cations which justifies the alkoxysilane functionalized nanopartices as selective, MEF-based sensors.

2.5. CONCLUSION

To summarize, EETMS concentration dependent synthesis of anisotropic palladium nanoparticles has been carried out. These nanoarrays produce significant changes in the fluorescence intensity of the probe molecules. The larger particles generate relatively higher signal enhancements than the smaller ones. The layers of alkoxysilanes acting as spacers regulate the separation between the metal surfaces and the fluorophores, considerably higher enhancements are recorded over large distances (around 300 – 400 nm). These further facilitate the spatial distribution and physisorption of molecules in the periphery of nanoparticles. Modulated near and far field interplay between the nanoparticle and the probe molecules, initiates the selectivity in behavior of palladium, silver and gold nanoarrays towards the variation in fluorescence emission intensity for different fluorophores (RhB, L-Trp and Fluorescein). Proximal interaction of the transient surface plasmons with emitter leads to a set of key changes in emission spectra, including the enhancement or reduction in intensity.